# GPU-BASED VISUALIZATION OF HYBRID TERRAIN MODELS

E. G. Paredes[1], M. Bóo[1], M. Amor[2], J. Döllner[3] and J. D. Bruguera[1]
[1]*Centro de Investigación en Tecnologías de la Información (CITIUS), University of Santiago de Compostela, Santiago de Compostela, Spain*
[2]*Dept. of Electronics and Systems, Univ. of A Coruña, A Coruña, Spain*
[3]*Hasso-Plattner-Institut, University of Potsdam, Potsdam, Germany*

Keywords: Hybrid Terrain Models, GPU Rendering, Terrain Visualization, Tessellation.

Abstract: Hybrid terrain models formed by a large regular mesh refined with detailed local TIN meshes represent an interesting and efficient approach for the representation of complex terrains. However, direct rendering of the component meshes would lead to overlapping geometries and discontinuities around their boundaries. The Hybrid Meshing algorithm solves this problem by generating an adaptive tessellation between the boundaries of the component meshes in real-time. In this paper, we present a highly parallel implementation of this algorithm using the Geometry Shader on the GPU.

## 1 INTRODUCTION

Interactive visualization of Digital Terrains Models (DTM) has been a common subject of research during the last decade. However, the integration of data from different sources is still a problematic question, although new data collections are constantly being created (Oosterom et al., 2008).

Hybrid terrain models present additional features for the representation of DTMs, not existing in the more common regular grid based Digital Elevation Models (DEM) or Triangulated Irregular Networks (TIN) models. Using hybrid models, a DTM can be defined by the combination of regular grid-based elevation data and some locally detailed TIN meshes of the complete terrain surface representing complex terrain features and artificial micro-structures like constructions or roads. Direct rendering of hybrid terrain models, however, could generate meshes with holes and geometric discontinuities between the borders of the different parts.

The Hybrid Meshing (HM) algorithm (Bóo et al., 2007) introduces a new method for combining the TIN and grid meshes in a new coherent crack-free model, for any LOD in the grid. This approach has recently been extended to support multiresolution rendering of both meshes (Paredes et al., shed).

In this paper, we present the GPU HM method, the first implementation of a hybrid model renderer working at interactive frame rates into the GPU. Based on the HM algorithm, our implementation uses Geometry Shader (GS) technology to attain parallelism by simultaneously running several GS threads performing the local tessellation of the models boundaries.

## 2 HM ALGORITHM

The HM algorithm achieves an efficient visualization of hybrid terrain models formed by a multiresolution regular grid and local high resolution TINs, as shown in previous works (Paredes et al., 2009). In Figure 1(c) is depicted an example of the crack-free model obtained from the union of the view-dependent refinement of a multiresolution grid (see Figure 1(a)) and a single-resolution TIN (see Figure 1(b)).

The algorithm joins the boundaries of both kind of meshes following a local tessellation strategy inside the multiresolution grid cells. The grid cells are classified as Non Covered (NC), Partially Covered (PC) or Completely Covered (CC) cells, according to the overlapping with the TIN mesh. During the visualization, the visible grid cells in the extracted view-dependent LOD of the grid are processed according to their classification. Thus NC cells are rendered as usual, CC grid cells are discarded since they will be replaced by the detailed TIN mesh, and PC cells are locally tessellated to join both meshes' boundaries.

To simplify the adaptive tessellation of the cells, the TIN boundary (TB) is locally convexified within

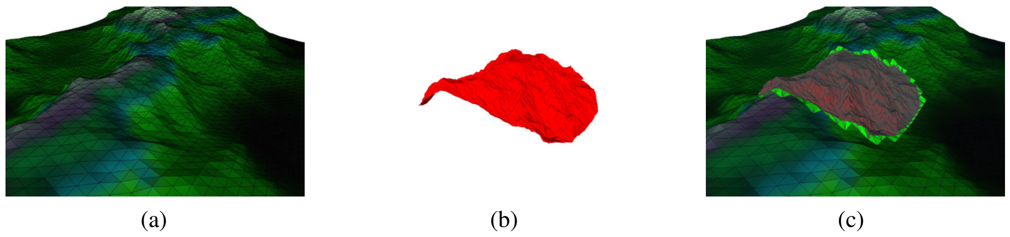

Figure 1: Hybrid terrain model example. (a) Base regular grid. (b) Detailed TIN component mesh. (c) Resulting hybrid model with different components highlighted.

each cell in a preprocessing stage, and the result encoded in a unified grid LOD independent representation. Thus, the convexification triangles are decoded during the visualization, while the remaining PC cells tessellation triangles are easily generated on-the-fly.

### 2.1 Local Tessellation Algorithm

Two precomputed data structures are used to connect the PC cell vertices and the convexified TIN boundary inside PC cells: the Grid Classification (GC) list and the list of PC cells (called Vertex Classification list in the original HM article and renamed here for reasons of clarity). The GC list stores the type (NC, CC, PC) of each cell in the multiresolution grid mesh. The list of PC cells contains the information used in the adaptive tessellation of each PC cell; i.e., the TB vertices whose 2D projection falls into the grid cell area, and the cell corner vertices not covered by the TIN mesh.

Since TB vertices and cell corner vertices are sequentially numbered, PC cell related data can be encoded as a 4-tuple $\{A, L, C, I\}$, where $A$ is the first TB vertex contained in the cell, $L$ is the number of TB vertices present in the cell, $C$ is the first corner vertex not covered by the TIN mesh, and $I$ is the number of uncovered corners in the cell. The cell tessellation is achieved by generating *corner triangles* joining consecutive TB vertices to the uncovered corners of the cell. Since the TB has been previously convexified (see Section 2.2), the cell corner vertices can be safely joined to consecutive TB vertices, shifting to the next cell used as link point with the TIN boundary, when the generated corner triangle overlaps the TIN.

### 2.2 Incremental Local Convexification of TIN Boundary

To easily regenerate on demand the convexification triangles for a given PC cell of any LOD, the HM algorithm precomputes and encodes these triangles using a unified representation valid for every grid LOD.

The process begins by computing the convexification of the TIN boundary in the PC cells at the

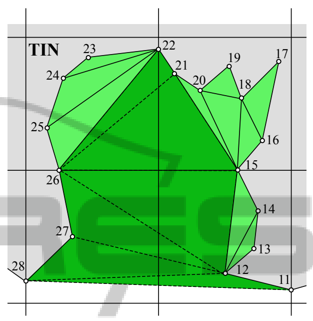

Figure 2: Incremental local convexification of the TB.

finest LOD. For each cell, the concave caves on the TB convex hull are detected and triangulated using any tessellation algorithm (Shewchuk, 1996). Figure 2 shows an example (represented in a top view) where the TB convex hulls of the PC cells are delimited by vertices $\{11, 12, 15\}$ (bottom right cell), $\{15, 21, 22\}$ (top right cell), $\{22, 26\}$ (top left cell) and $\{26, 27, 28\}$ (bottom left cell). Once the TIN boundary convexification at this LOD has finished, the same process is repeated at the next coarser LOD until the last one is reached. Since an incremental convexification strategy is used, triangles generated in this LOD are preserved in the convexification of the next coarser LOD. In the same example of Figure 2, the convex hull of the coarser level is defined by the vertices $\{11, 28\}$.

The TB list represents the TIN boundary vertices as a circular list stored in clockwise order. Associated to each boundary vertex there is an additional *connectivity* value indicating the distance, counted in number of vertices, between that vertex and the most distant one connected to it in the convexified TB. If vertex $i$ has a connectivity value $j$, the farthest boundary vertex connected to it in the convexified boundary is $i + j$. Also note that the starting vertex of a cave is connected to all the vertices in that cave, except for the ones forming part of a nested sub cave. This unified representation works perfectly well for different levels of detail, as explained in (Bóo et al., 2007).

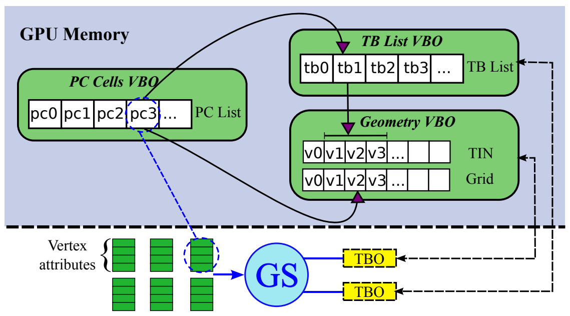

Figure 3: Organization of data structures in memory.

## 3 GPU HM APPROACH

Our approach attains the parallel tessellation of several PC cells by running multiple instances of the HM algorithm in the GPU cores. Furthermore, an optimized version of the original data structures is used to improve the memory access.

In our proposal, Geometry Shaders are used to decode the precomputed data structures and to generate the triangles needed for the tessellation of each PC cell. The GPU parallelism is automatically exploited as these tasks can be efficiently executed simultaneously in multicore GPUs.

Next, the optimized data structures and the tessellation and rendering algorithm are presented.

### 3.1 GPU and CPU Data Structures

The data structures used by the original HM algorithm were presented in Section 2: the GC list, the list of PC cells and the TB list. Since in the GPU HM method the rendering is performed by the Geometry Shader, every shader thread needs to access some of these structures and the meshes' geometric data. The original HM data layout, however, can not be efficiently accessed from the GPU. Thus, we have modified the data storage and accessing strategies depending upon their accessing pattern. Figure 3 illustrates the location and access methods used for the data structures.

The GC list is only needed to identify the coverage pattern of the cell for rendering the grid mesh. Once the grid cell has been identified, it is rendered, discarded or tessellated using the GPU and thus is not needed by the Geometry Shader.

The GPU HM rendering algorithm uses the geometric data of the TB vertices and the grid cell being tessellated, together with the TB data and the list of PC cells. Consequently, these data structures have to be maintained in GPU memory, stored in Vertex Buffer Objects (VBO), although they are accessed in different ways. The geometry data and the TB list need an array-like access, since the processing of one PC cell may involve reading non adjacent elements in random order. Texture Buffer Objects (TBO) (OpenGL.org, 2009), associated to the corresponding VBOs, are used in our proposal to read this data within the shader. Using TBOs is an efficient way to obtain array-like access to large data buffers in the GPU memory. They provide a convenient interface to the data, simulating a 1D texture where the tex coordinate corresponds to the offset in the buffer object. Additionally, accessing latencies can be effectively hidden by overlapping the readings with data processing operations, since in the HM rendering stage there are several processing operations.

An additional optimization to improve the data locality of the TB list has been used. The TIN mesh vertices are ordered in the vertex buffer containing the geometry data to guarantee that the TB boundary vertices are stored at the beginning. In this way, the offset of the vertex data in the buffer object represents its position in the TB list. Thus, vertex information can be accessed by using its TB index –reducing one level of indirection regarding to the original data structures– and adjacent vertices in the TB are now adjacent in the buffer object, improving the cache behavior due to this better data locality.

The PC list, on the other hand, is made available to the shader through normal input vertex attributes. There is a one-to-one relationship between PC cells and vertex shader threads; therefore, packing the items in the PC list as input vertex attributes is the most effective way to send the right information for every shader thread. Moreover, data transfer between CPU and GPU during rendering is reduced, given that we can use indexed draw calls to select the active PC cells being tessellated every frame. This list of active PC cells is easily built on-the-fly by the CPU according to the view-dependent grid LOD, and efficiently uploaded to the GPU due to its small size.

### 3.2 Rendering Algorithm

The GPU HM rendering steps are similar to the steps of the original algorithm, but the implementation differs. An overview of the render flow is presented in Figure 4 for a coarse (Subfigure 4(a)) and a fine (Subfigure 4(b)) grid LOD, following the order of the numerical labels. The TIN mesh is the same in both cases, but the PC grid cells depend on the grid LOD and thus different cells are rendered for each case. The first step of the process is to identify the *active* NC, CC, and PC cells. Next, the NC cells are rendered using indexed draw calls (step (1) in Figures

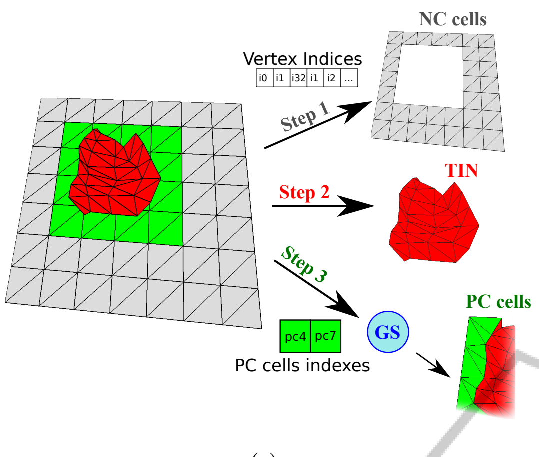

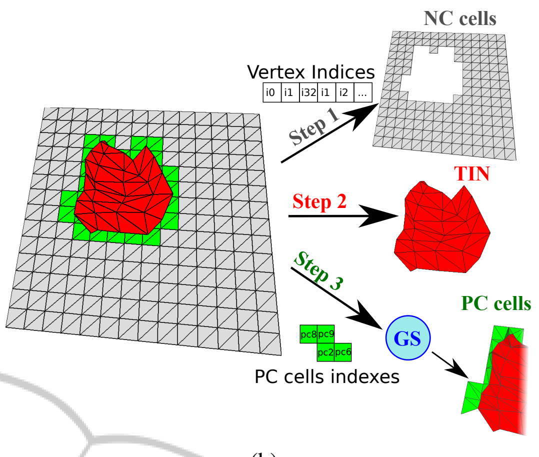

Figure 4: HM rendering algorithm steps. (a) Coarse LOD render. (b) Fine LOD render.

Table 1: Size of the test models.

| Model | Grid cells | TIN Δ | TB elems. |
|---|---|---|---|
| Coruña | 998K | 1739K | 17K |
| Sil | 998K | 657K | 14K |
| Pmouros | 998K | 656K | 16K |

4(a) and 4(b)), since geometry data is already stored in the GPU memory. CC cells are then replaced by the whole TIN mesh (step (2) in the same figures). This operation is lightweight since TIN meshes are static, usually cover around 20-30% of the grid extension, and the geometry data are also stored in the GPU memory, which makes the rendering very efficient.

Finally, the Geometry Shader which performs the PC cells adaptive tessellation is loaded and the list of active PC cells are sent to the GPU, where the actual tessellation is computed (step (3) in the same figures). The input of each shader thread is the tessellation data of the processed PC cell, encoding every data field in a different vertex attribute. By the time the Geometry Shader finishes the processing, all the convexification and corner triangles have been generated and the PC cell is completely tessellated.

During rendering, each one of the running Geometry Shader threads processes the TB vertices in the cell sequentially. The associated convexification triangles are reconstructed and emitted by the Geometry Shader, according to the algorithm presented in Subsection 2.2. Vertices belonging to the local convex hull of the TIN boundary are connected to the grid cell vertices, by generating additional corner triangles.

In the GPU HM, the sequential tessellation operations have been reordered and optimized for GPU execution. Several techniques have been applied, resulting in an implementation of the algorithm with fewer conditional branch statements, fewer loops and a reduced number of memory reading operations. The implementation strategy presented in (Bóo et al., 2007) shows that the decoding and generation of the incremental convexification triangles, and the generation of corner triangles are performed in two stages. We have succeeded in merging these different stages together, reducing the overall complexity of the source code and the number of conditional evaluations of our implementation.

Additional optimization techniques have been also used when possible, such as loop unrolling and transformation of complex conditional expressions into arithmetic expressions or several simpler expressions for faster evaluation. Another relevant performance improvement derives from the reordering of the TIN vertices in the vertex buffer. Due to this optimization, the data of a TB vertex is accessed with the same index and in the TB list and in the vertex buffer, eliminating the pointer to the geometry data position used in the original TB list. With this optimization, not only are data reading operation reduced to almost one half of the original number, but also many read operations in the same thread could benefit from data locality and attain much better cache behavior.

## 4 EXPERIMENTAL RESULTS

The results of our tests are shown in this section. The software application used for testing has been coded in C++. GLSL has been used in the shaders, since OpenGL is the hardware acceleration API. The performance results were collected in a Ubuntu Linux system with an Intel Core2 Quad 2.6 GHz processor. Two different Nvidia GeForce graphic cards, an GTX480 with 1.5GB of video memory and a GTX280

Table 2: Detailed description of the test models composition for each grid LOD.

| | | | | |
|---|---|---|---|---|
| | | *Coruña* | | |
| | L0 | L1 | L2 | L3 |
| PC cells | 517 (3.36%) | 1058 (1.71%) | 2142 (0.86%) | 4233 (0.43%) |
| NC cells | 14418 (93.77%) | 58606 (94.52%) | 236079 (94.81%) | 949668 (95.16%) |
| CC cells | 441 (2.87%) | 2337 (3.76%) | 10780 (4.33%) | 44100 (4.42%) |
| Rendered Δ | 1787K | 1876K | 2231K | 3661K |
| PC cells Δ | 19K (1,06%) | 19K (1,01%) | 20K (0,89%) | 22K (0,60%) |
| | | *Sil* | | |
| | L0 | L1 | L2 | L3 |
| PC cells | 857 (5.57%) | 1775 (2.86%) | 3510 (1.41%) | 7630 (0.76%) |
| NC cells | 13428 (87.33%) | 54666 (88.17%) | 217694 (87.43%) | 904681 (90.65%) |
| CC cells | 1091 (7.10%) | 5560 (8.97%) | 27797 (11.16%) | 85690 (7.10%) |
| Rendered Δ | 701K | 784K | 1111K | 2489K |
| PC cells Δ | 17K (2,38%) | 17K (2,17%) | 19K (1,66%) | 23K (0,90%) |
| | | *Pmouros* | | |
| | L0 | L1 | L2 | L3 |
| PC | 821 (5.34%) | 1697 (2.74%) | 3329(1.34%) | 7912 (0.79%) |
| NC | 13640 (88.71%) | 55752 (89.92%) | 225396 (90.52%) | 906434 (90.83%) |
| CC | 915 (5.95%) | 4552 (7.34%) | 20276 (8.14%) | 83655 (8.38%) |
| Rendered Δ | 704K | 804K | 1128K | 2497K |
| PC cells Δ | 20K (2,87%) | 36K (4,44%) | 20K (1,80%) | 27K (1,09%) |

with 1GB, were used in the tests.

Three sample models, depicted in Figure 5, were generated for testing purposes from freely available data in the Spanish GIS database (IDEE) (Infraestructura de Datos Espaciales de España (IDEE), 2002): *Coruña*, *Sil* and *Pmouros*. Table 1 contains the size of the sample models in terms of number of cells in the finest LOD of the grids, number of triangles in the TIN meshes, and number of vertices in the TB.

In Table 2, the number of PC, CC and NC cells are shown for each grid LOD from L0 − L3 (where L0 represents the coarsest level) as well as its ratio over the total number of cells. The last two rows show the total number of triangles used for rendering the model and the portion of them corresponding to the adaptive tessellation of the PC cells. Note that the *Coruña* model presents around twice the number of rendered triangles, as the TIN mesh is much higher detailed than the others.

The performance results of the GPU HM method are shown in Table 3. The table shows the averaged FPS obtained using the HM algorithm are presented in comparison to the FPS obtained rendering only the NC grid cells and the TIN mesh, which represents the maximum theoretical performance of the system. The relative performance penalty of our implementation is shown in parentheses. For each sample model, the tests results are divided according the active LOD in the grid ($L0 - L3$).

As can be seen in the results table, the overhead introduced by the GPU HM implementation does not prevent the rendering of large terrain models at interactive frame rates. The best performance results are obtained when the coarser LOD (L0) is selected. For finer LODs, performance tends to decrease, as the total number of rendered triangles is much higher. The cost of the HM algorithm implementation, however,

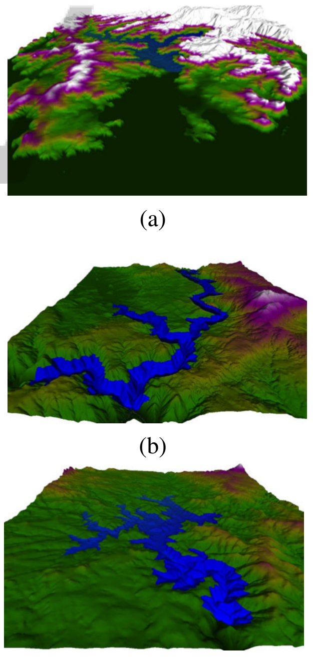

Figure 5: Hybrid models used in the tests with the TIN mesh highlighted in blue. (a) *Coruña* model. (b) *Sil* hybrid model. (c) *Pmouros* hybrid model.

Table 3: Performance results obtained with the HM algorithm, measured in FPS, using GTX480 and GTX280 GPUs.

| GTX 480 | | | | | |
|---|---|---|---|---|---|
| | Method | L0 | L1 | L2 | L3 |
| *Coruña* | NC + TIN | 330.90 | 319.73 | 283.64 | 192.91 |
| | HM | 232.20 (29.83%) | 233.62 (26.93%) | 213.31 (24.80%) | 155.42 (19.43%) |
| *Sil* | NC + TIN | 758.97 | 707.51 | 561.93 | 293.89 |
| | HM | 407.83 (46.27%) | 409.74 (42.09%) | 353.59 (37.08%) | 216.00 (26.50%) |
| *Pmouros* | NC + TIN | 813.42 | 754.78 | 591.35 | 313.56 |
| | HM | 276.58 (66.00%) | 256.32 (66.04%) | 348.41 (41.08%) | 210.86 (32.75%) |
| GTX 280 | | | | | |
| | Method | L0 | L1 | L2 | L3 |
| *Coruña* | NC + TIN | 90.30 | 87.99 | 79.15 | 62.02 |
| | HM | 76.06 (15.77%) | 87.61 (0.43%) | 78.99 (0.20%) | 61.82 (0.32%) |
| *Sil* | NC + TIN | 306.06 | 283.13 | 213.35 | 125.66 |
| | HM | 196.54 (35.78%) | 194.82 (31.19%) | 156.93 (26.44%) | 101.49 (19.23%) |
| *Pmouros* | NC + TIN | 354.43 | 322.90 | 233.64 | 134.77 |
| | HM | 142.74 (59.73%) | 148.63 (53.97%) | 159.75 (31.63%) | 94.43 (29.93%) |

is usually higher for coarser grid LODs, which have a low degree of parallelism. As shown in Table 2, the number of PC cells nearly doubles for consecutive finer LODs, while the number of PC tessellation triangles rises only marginally. Since a new parallel thread is used for the tessellation of a PC cell, this difference in the number of PC cells directly affects to the degree of parallelism in the implementation, and thus the global performance.

This also explains the noticeable larger performance penalty when using the more powerful GTX 480 graphic card (480 cores) compared to the GTX 280 (280 cores). Although the absolute performance is still much better using the GTX 480, the relative performance of the HM algorithm is worse, since the GTX 480 has a larger number of cores and thus fewer threads are being executed by each core. However, this effect is only important at very high frame rates and thus it does not limit the validity of our implementation. For example, our system is able to render the largest test model, *Coruña bay*, at the maximum available detail (roughly 3.7 millions of triangles) at 155 FPS using the GTX480 card.

## 5 CONCLUSIONS

The HM algorithm is an efficient solution for rendering hybrid terrain models formed by a base multiresolution grid mesh and high-resolution TINs. In this paper we have presented a new implementation of the method based on Geometry Shaders. Due to this shader based approach, our implementation is easy to integrate with any modern rendering pipeline.

This GPU implementation of the HM algorithm is formed by two phases, like the original algorithm.

The harder computations are performed in the preprocessing phase, and encoded in simple data structures. During the rendering, the GPU decodes these structures and generates the adaptive tessellation at the same time, joining the component meshes.

The performance of the method, as well as the quality of the rendered hybrid models has been demonstrated in our experiments. Our implementation manages to render models of several millions of triangles, without geometric discontinuities or overlapping, at interactive frame rates. To our knowledge, no other hybrid terrain rendering algorithm has been implemented using GPUs.

## REFERENCES

Bóo, M., Amor, M., and Döllner, J. (2007). Unified hybrid terrain representation based on local convexifications. *GeoInformatica*, 11(3):331–357.

Infraestructura de Datos Espaciales de España (IDEE) (2002). Digital elevation models. http://www.idee.es.

Oosterom, P. v., Zlatanova, S., Penninga, F., and Fendel, E. (2008). *Advances in 3D Geoinformation Systems*. Lecture Notes in Geoinformation and Cartography. Springer Berlin.

OpenGL.org (2009). OpenGL Texture Buffer Object ext.

Paredes, E. G., Bóo, M., Amor, M., Bruguera, J. D., and Döellner, J. (To be published). Extended hybrid meshing algorithm for multiresolution terrain models. *Int. Journal of Geographic Information Science*.

Paredes, E. G., Lema, C., Amor, M., and Bóo, M. (2009). Hybrid terrain visualization based on local tessellations. In *GRAPP 09: Procs. of the Int. Conf. on Comp. Graphics Theory and Applications*. SciTePress.

Shewchuk, J. (1996). Triangle: Engineering a 2D quality mesh generator and Delaunay triangulator. *Lecture notes in Computer Science*, 1148:203–222.